ELSEVIER

Physics of the Earth and Planetary Interiors 107 (1998) 221–231

PHYSICS OF THE EARTH AND PLANETARY INTERIORS

Decomposition of K-amphibole at high pressures and implications for subduction zone volcanism

Toru Inoue [a,*], Tetsuo Irifune [a], Hisayoshi Yurimoto [b], Isoji Miyagi [b,1]

[a] *Department of Earth Sciences, Ehime University, 2-5 Bunkyo-cho, Matsuyama 790, Japan*
[b] *Earth and Planetary Sciences, Tokyo Institute of Technology, 2-12-1 Ookayama, Meguro-ku, Tokyo 152, Japan*

Received 14 August 1995; revised 20 May 1996; accepted 15 June 1996

Abstract

The stability of K-amphibole has been studied at pressures 12.6–16.5 GPa, and at temperatures 940–1450°C. K-amphibole decomposes into an assemblage of clinoenstatite + diopside + an unknown phase (X) + stishovite + fluid at pressures above 16 GPa and temperatures below 1200°C. The phase boundary has a negative Clapeyron slope, and the high temperature assemblage is clinoenstatite + diopside + X + wadeite-type $K_2Si_4O_9$ + fluid at pressures 14–16 GPa. The X phase has a cation ratio of approximately K:Mg:Si = 1:2:2, and contains 1.7 ± 0.1 wt.% H_2O as determined by SIMS measurements, leading to a formula of $K_4Mg_8Si_8O_{25}(OH)_2$. The present results suggest that the decomposition of K-amphibole in the dragged hydrous peridotite layer at the base of the mantle wedge may produce certain amounts of H_2O-rich fluid at 14–16 GPa ($\sim$ 450 km depth), while some of H_2O is trapped in the new hydrous phase X and is further carried into deeper regions of the mantle. The aqueous fluid released by the decomposition of K-amphibole should react with β-phase to form hydrous β-phase in the mantle transition region. Thus, the dehydration of K-amphibole would not cause any volcanic activities in the back arc regions, in contrast to the dehydrations of amphibole, chlorite and phlogopite, which are presumably responsible for the first and the second volcanic chains. However, some of the volcanic activities such as in Muriah, Indonesia, may be related to the dehydration of K-amphibole in unusually hot regions above the subducting slab.

Keywords: K-amphibole; Subduction zone volcanism; Decomposition

1. Introduction

The presence of H_2O has some important bearings on the constitution and dynamic processes of the earth's mantle via the phenomena such as changes in melting relations of mantle materials, transportation of chemical species by aqueous fluids, changes in rheological properties, etc. The inventory of H_2O in the mantle partly comes from the dehydration of hydrous minerals at high pressure that constitute a subducting slab or dragged hydrous peridotite present at the interface between the mantle wedge and the slab.

Tatsumi (1989) proposed that the hydrous peridotites dragged downward on the slab surface are

* Corresponding author.
[1] Present address: Geological Survey of Japan, 1-1-3 Higashi, Tsukuba, Ibaraki 305, Japan.

0031-9201/98/$19.00
PII S0031-9201(97)00135-0

dehydrated at certain depths and release H_2O which migrates upwards to cause melting of mantle wedge peridotite. The dehydrations of amphibole and chlorite occur at relatively low pressures, and are probably related to the trench-side (i.e., first) volcanic chain located at ~110 km above the Benioff zone, while the backarc-side (i.e., second) chain may be caused by the released H_2O upon the dehydration of phlogopite at a deeper (~180 km) level. Moreover, the presence of further backarc-side (i.e., third) volcanism is suggested in certain locations, i.e., Muriah, Indonesia (Edwards et al., 1991) and Kamchatka (Tatsumi et al., 1994), which is supposed to be caused either by the dehydration of K-amphibole or partial melting of K-amphibole bearing peridotite that persists to higher pressures compared to other hydrous phases mentioned above.

Tronnes et al. (1988) and Sudo and Tatsumi (1990) studied the stability of K-amphibole at high pressures and high temperatures. K-amphibole was found to be formed at the expense of phlogopite + pyroxenes in the peridotite plus phlogopite assemblage or as the decomposition product of phlogopite + diopside. K-amphibole thus synthesized was stable at pressures to 14 GPa, at temperatures 1000–1200°C. The stability of K-amphibole at higher pressures should be further studied experimentally to address the relation between the existence of the third volcanism and the dehydration of K-amphibole.

The purpose of the present study was determine the stability limit of K-amphibole at high pressure. Characterization of the high-pressure phases was also conducted with special attention to the nature of the hydrous phase which might be present as the post K-amphibole phase. The cause of the possible third chain volcanism is discussed on the basis of the present experimental data.

2. Experimental methods

2.1. Starting material

First, we prepared a mixture of oxides and carbonates of the K-amphibole ($K_2CaMg_5Si_8O_{22}(OH)_2$) minus brucite ($Mg(OH)_2$) composition. A mixture of K_2CO_3, $CaCO_3$, 4MgO and $8SiO_2$ was ground under acetone in an agate mortar and sintered in an oven at 1100°C for 24 h. X-ray diffraction and EPMA analyses showed that the product consisted of diopside plus glass. Then, the product was finely ground and mixed with brucite in an appropriate proportion. Thus, H_2O was supplied via brucite without addition of any free water to the starting mixture. The starting mixture was sealed in Pt capsules in the same manner as adopted in our previous work (Inoue and Sawamoto, 1992). The outer diameters of the capsules were 1.7 mm, and the lengths were less than 1.5 mm.

2.2. High pressure and high temperature techniques

The high-pressure experiments were performed in an MA8-type apparatus. We used truncation edge lengths (TEL) of 5.0 and 3.5 mm for the second stage anvils. For the experiments up to 14.7 GPa, an 11-mm edge octahedron of semi-sintered MgO was used as a pressure medium for the TEL = 5.0 mm system. A cylindrical graphite or tantalum heater was used according to the pressures studied, because graphite dose not work as a heater owing to rapid transformation to diamond at pressures greater than 14 GPa in the present temperature interval. In order to reduce heat loss by thermal radiation, 5 wt.% of CoO was doped in the MgO pressure medium. For the experiments up to 16.5 GPa, we used an octahedral pressure medium of 9.5-mm edge length using the anvils of TEL = 3.5 mm. In this pressure range, we only used platinum as a heating element. The cell assembly used in the present study is schematically illustrated in Fig. 1.

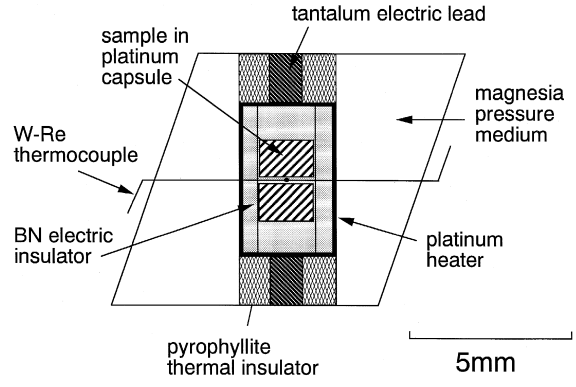

Fig. 1. A schematical illustration of the cross-section of the cell assembly used in the present study.

Fig. 2 shows the pressure calibration curves used in the present study. The pressure was calibrated by means of the following phase transitions at room temperature: low Bi (2.55 GPa), high Bi (7.7 ± 0.3 GPa), ZnS (15.5 ± 0.7 GPa), and GaAs (18.7 ± 0.7 GPa). In addition, we have performed pressure calibrations at a high temperature (1200°C) for the system of TEL = 3.5 mm, using the coesite-stishovite transition in SiO_2 (9.5 GPa, Akaogi and Navrotsky, 1984), and the α–β transition in Mg_2SiO_4 (14 GPa; Akaogi et al., 1989). We also checked the pressure at this temperature by measuring the compositions of coexisting β- and γ-phases using a composition of $(Mg_{0.9}Fe_{0.1})_2SiO_4$ (16.5 GPa; Akaogi et al., 1989). The pressure at high temperature was lower by about 6% from that at the room temperature. The pressures at high temperature for the system TEL = 5.0 mm was also examined using the compositions of coexisting α- and β-phases in $(Mg_{0.9}Fe_{0.1})_2SiO_4$. The reduction of pressure at high temperature was almost the same amount as observed in the system TEL = 3.5 mm.

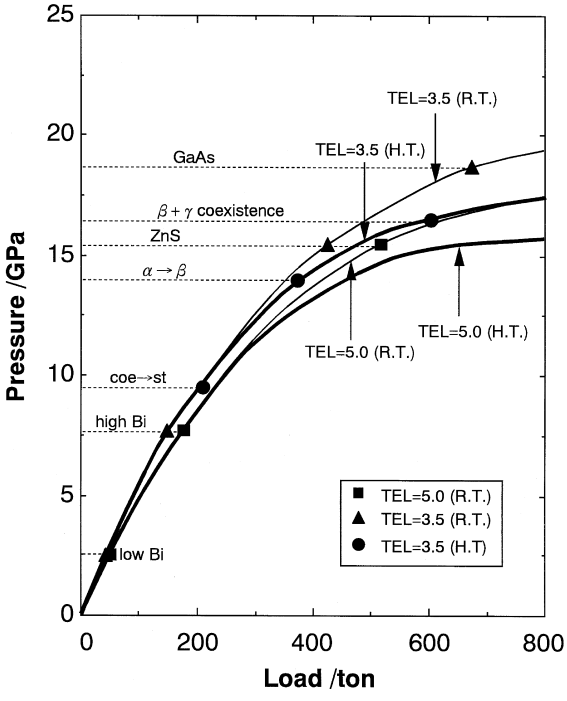

Fig. 2. Pressure calibration curves for the multi-anvil apparatus with truncated edge lengths of 3.5 mm (TEL = 3.5) and 5.0 mm (TEL = 5.0). Thin lines represent the calibration curves at room temperatures, while the thick lines are those at a temperature of 1200°C.

Temperatures were measured with W3%Re–W25%Re thermocouples, whose cold junctions were connected to the anvil surface. The temperatures of the anvil surface were measured with chromel–alumel thermocouples, which were used for the temperature correction. No pressure correction was made for the e.m.f. of the thermocouple. During each run, temperature was kept constant within ±10°C and pressure was maintained at a constant load. The run was then quenched by shutting off the electric power.

In these experiments, the temperature gradients in the capsules were not measured directly. However, we believe that the gradients in the capsules were less than 150°C from previous experiments (Inoue, 1994) and the evaluation of the temperature distribution in these furnaces using pyroxene geothermometry (Mizobuchi et al., unpublished data). Nevertheless, we carefully selected the sample only near the thermocouple for examination.

2.3. Examination of run products

For all runs, polished sections of the recovered run products were examined by a scanning electron microscope (SEM) and an electron microprobe analyzer with both wavelength dispersive and energy dispersive systems. The polished samples were also examined using a microfocus (30 ~ 100 μm) X-ray diffractometer, while some of the samples were analyzed by the conventional X-ray powder diffraction method. The lattice parameters of the present K-amphibole were determined by a least square refinement using 27 reflections with CuKa1 radiation.

For quantitative analyses of the amount of H in the unknown hydrous phase, we used secondary ion mass spectroscopy (SIMS; Cameca IMS-3F) at Tokyo Institute of Technology. A primary beam operated at 10 nA, 12.5 kV $^{16}O^-$ was focused to form a 30-μm spot on the sample, and the secondary $^1H^+$ and $^{30}Si^+$ ions were collected from the central region (10 μm in diameter) of the spattered area. For quantitative analysis, a natural amphibole specimen possessing 1.66 wt.% of H_2O (Miyagi and Yurimoto, 1995) was used as a standard material. The amount of H in unknown samples was determined using a linear

relationship between the H_2O concentration and H/Si ratio in the SIMS measurements (Yurimoto et al., 1989).

3. Experimental results

3.1. Phase relationship

The experimental conditions and the results are summarized in Table 1 and plotted on a P–T diagram in Fig. 3. The results for the system phlogopite plus diopside (Sudo and Tatsumi, 1990) are also depicted in Fig. 3. K-amphibole was found to be stable at pressures up to 16 GPa, at temperatures below 1200°C. The powder X-ray diffraction data of the present K-amphibole is consistent with that of $KNaCaMg_5Si_8O_{22}(OH)_2$ richterite reported by Huebner and Papike (1970). The lattice parameters calculated using the reflections listed in Table 2 are $a = 10.180(8)$ Å, $b = 18.078(12)$ Å, $c = 5.285(6)$ Å, $\beta = 105.17(8)°$, $V = 938.7(14)$ Å^3. The *a*-, *b*-, and *c*-axes are larger by about 1.3, 0.5, and 0.2%, respectively, as compared to those of $KNaCaMg_5Si_8O_{22}(OH)_2$ richterite (Huebner and Papike, 1970). The slight expansion of the unit cell dimensions is presumably due to the replacement of Na by K in the present K-amphibole.

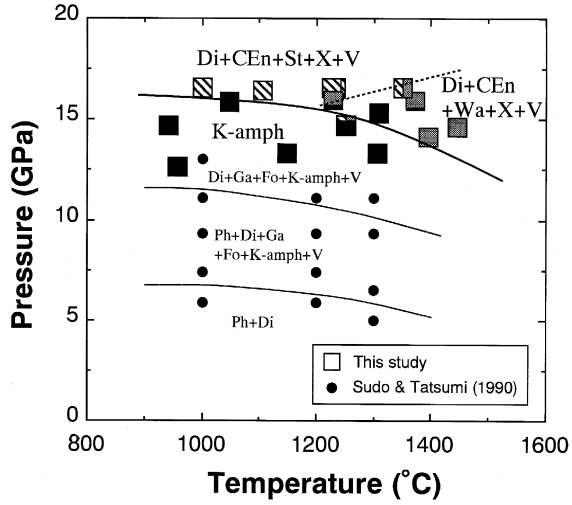

Fig. 3. A phase diagram for the K-amphibole composition based on the present experiments. The phase relationship for the system phlogopite + diopside is also illustrated (thin curves) on the basis of Sudo and Tatsumi (1990). K-amph: K-amphibole; Di: diopside; CEn: clinoenstatite; St: stishovite; Wa: $K_2Si_4O_9$ wadeite; X: unknown phase; V: quenched vapor; Ph: phlogpite; Ga: garnet; Fo: forsterite.

At higher pressures, and at temperatures below 1200°C, K-amphibole decomposes into an assemblage of diopside + clinoenstatite + stishovite + an

Table 1
Experimental conditions and results

Run N	Press. (GPa)	Temp. (°C)	Time (min)	Results
940621K	12.6	960	60	K-amph(+St + Di)
940630K	13.4	1150	60	K-amph(+St)
940711K	13.4	1310	60	K-amph(+Di + CEn)
940706K	14.1	1400	30	Di + CEn + Wa + X
940719K	14.7	940	40	K-amph
940805K	14.7	1250	30	K-amph(+Di + CEn + St + Wa + X)
940811K	14.7	1445	45	Di + CEn + Wa + X
950303K	15.3	1310	30	K-amph(+Di)
940909K	15.9	1050	35	K-amph(+Di + CEn)
940831K	15.9	1225	40	Di + CEn + Wa + X + K-amph
940913K	15.9	1370	30	Di + CEn + Wa + X(+K-amph)
941102K	16.5	1000	40	Di + CEn + St + X
940921K	16.5	1105	40	Di + CEn + St + X
950220K	16.5	1220	60	Di + CEn + St + X
941214K	16.5	1230	60	Di + CEn + St + X(+K-amph)
941027K	16.5	1350	3	Di + CEn + St + Wa + X

Pressures were calibrated at high temperature (1200°C).
K-amph: K-amphibole; St: stishovite; Di: diopside; CEn: clinoenstatite; Wa: $K_2Si_4O_9$ wadeite; X: unknown phase.
Phases in parentheses are very minor in quantity and detected only by careful examinations using EPMA.

Table 2
XRD data for the present K-amphibole synthesized in run 940909K

d_{obs} (Å)	d_{calc} (Å)	I/I_{100}	h	k	l
8.60	8.63	30	1	1	0
4.90	4.91	12	−1	1	1
4.53	4.52	15	0	4	0
3.98	3.90	18	−1	3	1
3.383	3.394	78	1	3	1
3.325	3.326	100	−2	4	0
3.219	3.222	61	3	1	0
2.988	2.975	24	2	2	1
2.953	2.950	87	−1	5	1
2.875	2.877	38	3	3	0
2.802	2.796	55	−3	3	1
2.709	2.714	82	1	5	1
2.595	2.594	41	0	6	1
2.551	2.553	86	−2	0	2
2.429	2.427	36	3	5	0
2.397	2.392	32	−4	2	1
2.380	2.378	27	−3	5	1
2.308	2.310	38	−3	1	2
2.223	2.223	21	−2	4	2
2.175	2.177	41	2	6	1
2.059	2.054	15	2	0	2
2.040	2.058	24	−4	0	2
1.953	1.953	30	5	1	0
1.867	1.869	19	−1	9	1
1.673	1.675	36	4	6	1
1.663	1.663	22	−4	8	0
1.623	1.620	16	1	11	0

unknown phase (X) (+vapor). At higher temperatures, however, wadeite-type $K_2Si_4O_9$ formed while stishovite disappeared from this assemblage. The presence of the X phase was confirmed by both electron microprobe analysis and X-ray diffraction method. It was difficult, however, to obtain a complete set of diffraction peaks for this phase, as there were a number of other peaks from the coexisting phases. Careful examination using a microfocus diffractometer (~30-μm beam diameter) suggested that the following *d*-values correspond to this phase, though we were unable to obtain reliable relative intensities due to the preferred orientation of a few relatively large (~10 μm) grains; $d = 3.12$, 2.74, 2.363, 2.273, 2.115, 1.964, 1.184, 1.133, 0.900, 0.876 Å.

The phase boundary between K-amphibole and the high-pressure phase assemblages has a negative Clapeyron slope, almost parallel to the phase boundaries at low pressures for the phlogopite + diopside composition (Sudo and Tatsumi, 1990). The boundary between the two high-pressure phase assem-

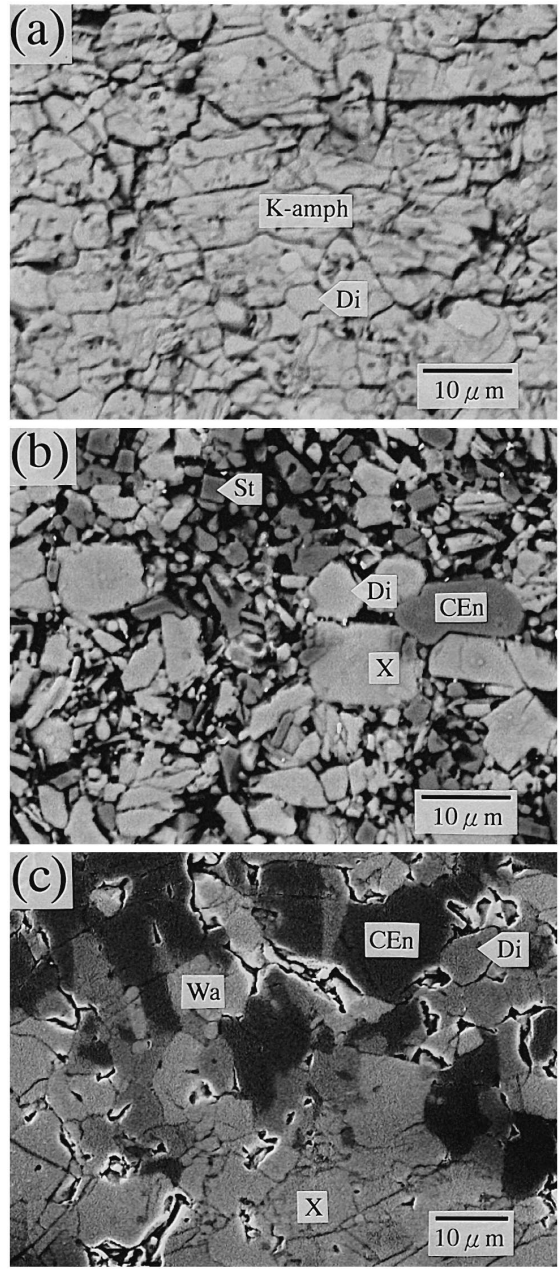

Fig. 4. Back-scattered electron images of the products from (a) run 940805K (14.7 GPa, 1250°C), (b) run 950220K (16.5 GPa, 1220°C) and (c) run 940811K (14.7 GPa, 1445°C). Abbreviations are the same as in Table 1.

Table 3
Representative chemical compositions of the coexisting phases

	940711K (13.4 GPa, 1310°C)	940805K (14.7 GPa, 1250°C)	940811K (14.7 GPa, 1445°C)				950220K (16.5 GPa, 1220°C)				940913K (15.9 GPa, 1370°C)					941027K (16.5 GPa, 1350°C)				
	K-amph	K-amph	Di	CEn	Wa	X	Di	CEn	St	X	K-amph	Di	CEn	Wa	X	Di	CEn	Wa	St	X
MgO	23.52	23.41	24.98	40.04	0.06	31.64	20.65	39.20	0.45	30.35	23.00	20.21	39.04	0.39	31.18	21.80	39.82	0.13	0.29	29.81
SiO_2	55.83	56.95	57.75	61.05	72.87	49.95	56.58	59.57	97.86	47.25	56.17	54.06	59.69	72.44	47.51	55.15	59.17	72.00	100.81	46.63
K_2O	10.84	10.24	0.65	0.04	26.82	16.42	0.45	0.25	0.27	19.40	10.04	0.53	0.15	27.19	17.61	0.08	0.02	27.53	0.00	17.24
CaO	6.88	6.50	18.08	0.77	0.15	0.16	22.84	0.28	0.00	0.35	6.66	22.55	0.39	0.28	0.09	20.42	0.27	0.30	0.00	0.17
Total	97.07	97.10	101.45	101.90	99.90	98.17	100.52	99.29	98.58	97.35	95.87	97.35	99.27	100.30	96.39	97.45	99.29	99.95	101.10	93.85
Oxygen N	23	23	12	12	9	12	12	12	12	12	23	12	12	9	12	12	12	9	12	12
Mg	5.00	4.95	2.59	3.92	0.00	3.59	2.19	3.94	0.04	3.56	4.93	2.22	3.92	0.03	3.65	2.37	4.00	0.00	0.03	3.58
Si	7.97	8.07	4.02	4.01	4.02	3.80	4.02	4.02	5.97	3.72	8.07	3.99	4.02	4.00	3.73	4.02	3.99	4.00	5.99	3.76
K	1.97	1.86	0.06	0.00	1.89	1.59	0.04	0.02	0.02	1.95	1.84	0.05	0.01	1.91	1.77	0.01	0.00	1.95	0.00	1.77
Ca	1.05	0.98	1.35	0.05	0.01	0.01	1.74	0.02	0.00	0.03	1.02	1.78	0.03	0.01	0.01	1.59	0.02	0.01	0.00	0.01
Cation sum	15.99	15.86	8.01	7.98	5.92	8.99	7.99	8.00	6.03	9.26	15.86	8.04	7.98	5.95	9.16	7.99	8.01	5.96	6.01	9.12

blages of K-amphibole seems to have a positive Clapeyron slope, though this has not been well constrained by the present experiments. It should be noted that there is no evidence of melting of K-amphibole at temperatures up to 1310°C in the present pressure range. The high-pressure phases also remained unmelted at temperatures up to about 1450°C as shown in the following section.

3.2. Crystal morphology

The back scatter electron images of the run products at (a) 15.3 GPa, 1310°C, (b) 16.5 GPa, 1220°C, and (c) 14.7 GPa, 1445°C are shown in Fig. 4. K-amphibole exhibited prismatic and subhedral to anhedral morphology, indicating that this amphibole is not a quenched product from melt.

The decomposition product of K-amphibole at 16.5 GPa, at 1220°C, also exhibited subhedral to euhedral morphology as shown in Fig. 4b. Clinoenstatite and the unknown phase crystallized to relatively large ($\sim 10\ \mu$m) crystals, while the grain sizes of stishovite and diopside crystals were normally less than 5 μm. The quenched vapor was difficult to identify from these textural observations. However, mass-balance considerations and the porous nature of the thin sections shown in Fig. 4 suggest that the vapor phase should have existed in the run products.

Fig. 4c shows a back-scattered electron image of the decomposition product at a higher temperature of 1445°C. At this temperature, wadeite form of $K_2Si_4O_9$ replaces stishovite in the lower temperature assemblage. Coexistence of four phases, i.e., clinoenstatite, diopside, X, and wadeite is clearly seen in Fig. 4. These phases crystallized to larger ($\sim 10\ \mu$m) grains as compared to those obtained at lower temperatures (Fig. 4b).

3.3. Phase chemistry

The chemical compositions of the coexisting phases are shown in Table 3. K-amphibole has a composition close to $K_2CaMg_5Si_8O_{22}(OH)_2$, which does not change significantly in all of the present runs. Wadeite and stishovite have almost ideal compositions of $K_2Si_4O_9$ and SiO_2, respectively.

Clinoenstatite has a composition of essentially pure $MgSiO_3$ in all of the present runs, while diopside contains appreciable amounts of the excess Mg-component (i.e., $Mg/(Mg + Ca) > 0.5$) in these runs. The Mg-component in diopside increased with increasing temperature, which agrees with the experimental results on the enstatite–diopside join studied by Gasparik (1990). This consistency suggests that our runs were in chemical equilibrium.

The X phase possesses a cation ratio of approximately Mg:Si:K = 2:2:1 and has no notable amount of calcium ions. The deficits of the oxide totals in the microprobe analyses suggest that this phase may have a few wt.% of H_2O. The SIMS measurements demonstrated that this phase actually contains 1.7 ± 0.1 wt.% H_2O, leading to an approximate formula of $K_4Mg_8Si_8O_{25}(OH)_2$.

4. Discussion

4.1. Decomposition of K-amphibole at high pressure

As shown in Section 3, K-amphibole decomposes into a phase assemblage of diopside + clinoenstatite + X + stishovite + fluid at pressures above 16 GPa and at temperatures below 1200°C, while an alternative assemblage of diopside + clinoenstatite + X + wadeite + fluid is encountered at higher temperatures, at pressures above 14–15 GPa. On the basis of the chemical compositions and phase assemblages determined in the present study, the decomposition of K-amphibole may be governed by the following idealized reactions:

$(T < 1200°C)$

$$2K_2CaMg_5Si_8O_{22}(OH)_2 = 2MgCaSi_2O_6$$

K-amphibole — diopside

$$+ 8nMgSiO_3 + 4SiO_2$$

clinoenstatite, stishovite

$$+ (1-n)K_4Mg_8Si_8O_{25}(OH)_2$$

X

$$+ (1+n)H_2O \cdot 2nK_2O$$

fluid

$(T > 1200°C)$

$$4K_2CaMg_5Si_8O_{22}(OH)_2 = 4MgCaSi_2O_6$$
K-amphibole diopside
$$+8(1+m)MgSiO_3 + 2K_2Si_4O_9$$
clinoenstatite wadeite
$$+(1-m)K_4Mg_8Si_8O_{25}(OH)_2$$
X
$$+(3+m)H_2O\cdot 2mK_2O$$
fluid

where n and m are the values between 0 and 1. We were unable to determine the compositions of quenched vapors (fluids) in the present experiments as mentioned in the earlier section. We then assume the fluids are mainly composed of H_2O and K_2O, because it was demonstrated that a large amount of K_2O is dissolved in aqueous fluid as compared to other chemical species; the K_2O concentration in H_2O (g/100 g H_2O) were reported as 4 at 1.1 GPa, 7 at 2 GPa and 25 at 3 GPa, respectively (Ryabchikov and Boettcher, 1980). Thus, there is a large pressure dependence of the solubility of K_2O in the aqueous fluid. When we assume that the K_2O concentration is 100 at the present experimental pressures, the values of n and m may be about 0.1 and 0.3, respectively. This indicates that H_2O-rich fluids of 2 ~ 3 wt.% may be released upon the decomposition of K-amphibole at 14–16 GPa.

In order to understand the stability of K-amphibole in the upper mantle, the effect of olivine on the stability of K-amphibole should be taken into account. If olivine is added to K-amphibole, the following reaction may occur:

$$2K_2CaMg_5Si_8O_{22}(OH)_2 + 4Mg_2SiO_4$$
K-amphibole β-phase
$$= 2MgCaSi_2O_6 + 8(1+p)MgSiO_3$$
diopside clinoenstatite
$$+(1-p)K_4Mg_8Si_8O_{25}(OH)_2$$
X
$$+(1+p)H_2O\cdot 2pK_2O$$
fluid

where p is the value between 0 and 1.

Comparing the reactions (1) and (2) with (3), only stishovite and wadeite of the decomposed products are involved in the reactions with olivine to form clinoenstatite as follows:

$$Mg_2SiO_4 + SiO_2 = 2MgSiO_3$$
β-phase stishovite clinoenstatite
$$4Mg_2SiO_4 + K_2Si_4O_9 = 8MgSiO_3 + K_2O$$
β-phase wadeite clinoenstatite fluid.

Thus, it is unlikely that the coexistence of olivine alters the decomposition boundary of K-amphibole. In fact, K-amphibole can coexist with olivine at least to 13 GPa and 1000°C (Sudo and Tatsumi, 1990). It should be stressed that reactions (1), (2) and (3) are univariant, i.e., K-amphibole decomposes at a certain depth in the mantle.

4.2. Implications for the transportation of H_2O into the deep mantle and the origin of the third volcanic chain

Fig. 5 shows the phase boundary between K-amphibole and the high-pressure phases determined in the present study. The phase boundary for the decomposition of phlogopite + diopside (Sudo and

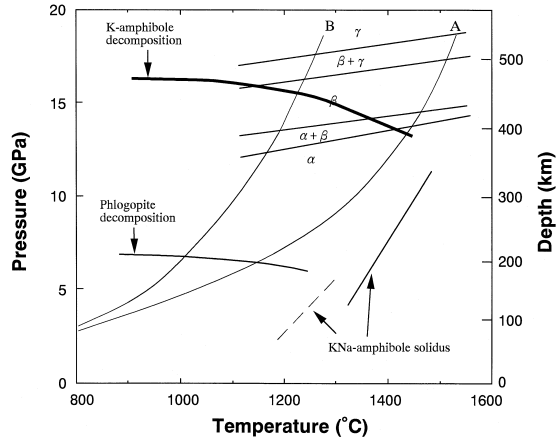

Fig. 5. Stability of K-amphibole, which is formed by the decomposition of phlogopite (Sudo and Tatsumi, 1990) and further decomposes to high pressure phases as shown in Fig. 3. The solidus lines for the KNa-amphibole are also illustrated on the basis of Tronnes et al. (1988) (solid line) and Foley (1991) (broken line), and the stability fields of $(Mg_{0.89}Fe_{0.11})_2SiO_4$ (in α-, β- and γ-forms) on the basis of Katsura and Ito (1989). Curve A represents a typical mantle geotherm by Ito and Katsura (1989), while B represents a typical temperature profile at the surface of the subducting slab according to Honda and Uyeda (1983).

Tatsumi, 1990), the solidus curve of KNa-amphibole (Tronnes et al., 1988; Foley, 1991), and the phase relations for $(Mg_{0.89}Fe_{0.11})_2SiO_4$ (Katsura and Ito, 1989) are also depicted in Fig. 5.

The curves A and B denote a representative mantle geotherm (Ito and Katsura, 1989) and a typical temperature profile for the upper surface layer of the subducting slab (Honda and Uyeda, 1983), respectively. The temperatures of the mantle wedge adjacent to the subducting slabs may be something in between these two temperature profiles. The decomposition boundary of phlogopite intersects these temperatures at depths close to 170–180 km, where the released aqueous fluid may cause the second volcanic chain at the back arc regions (Tatsumi, 1989).

It is noteworthy that the decomposition of K-amphibole occurs at the temperature and pressure conditions corresponding to the upper part of the mantle transition region, where the β-phase of olivine is believed to be the most abundant mineral phase. It has been demonstrated that this phase can accommodate up to 3.3 wt.% H_2O (Inoue et al., 1995), and a few weight percent of released H_2O upon decomposition of K-amphibole should react with the β-phase to form hydrous β-phase. It follows that the aqueous fluid generated by the dehydration of K-amphibole is completely consumed in the mantle transition zone and would not be transported to the shallower depths. Thus, there is fundamental deference in the role of the decomposition of hydrous phases at various depths; the occurrence of aqueous fluids due to the dehydrations of amphibole/chlorite and phlogopite may be responsible for the first and second volcanic chains as discussed by Tatsumi (1989), whereas no such fluids are available in the mantle transition region deeper than 400 km and the dehydration of K-amphibole is unlikely mechanism to cause the 'third volcanic chain'.

The presence of the third chain volcanisms is suggested in Kamchatka and Muriah (Indonesia) areas, which lie 300 km (Tatsumi et al., 1994) and 370 km (Edwards et al., 1991) above the Benioff zone, respectively. The present experimental results suggest that the volcanism in the latter area may be related to the dehydration of K-amphibole if the temperatures beneath this area are close to the typical mantle geotherm (Fig. 5A). K-amphibole decomposes to high-pressure phases at the pressures that correspond to the depths of about 380 km, releasing certain amount of aqueous fluid. At these depths, olivine remains in the α-form, which accommodates virtually no H_2O in its crystal structure. Thus, the dehydrated H_2O may be present as aqueous fluids at these depths and would migrate upward in the mantle wedge to produce magma by depressing melting temperature of the mantle peridotite. The high K_2O contents (average $\sim$5 wt.%, max. $\sim$9 wt.%) of the Muriah volcanos (Edwards et al., 1991) may be due to the K-bearing fluids thus generated by the dehydration of K-amphibole.

On the other hand, the third chain volcanism of Kamchatka does not appear to be related to the dehydration of K-amphibole, as the depth to the Benioff zone ($\sim$300 km) is significantly shallower than the stability limit of K-amphibole, as shown in Fig. 5. The volcanic activity in this area may be caused by partial melting of K-amphibole bearing peridotite under anomalously high temperature condition as discussed by Tatsumi et al. (1994). However, the present results and those of Tronnes et al. (1988) and Foley (1991) suggest that K-rich amphibole may have a quite high melting temperature of about 1450°C at a depth of 300 km, and it is unclear whether K-amphibole in hydrous peridotite can melt under these conditions. Thus, further studies of the melting relations of K-amphibole are required to evaluate this hypothesis advocated by Tatsumi et al. (1994).

A schematic illustration of the subduction related volcanism is shown in Fig. 6. Tatsumi (1989) presents a plausible model for the migration of H_2O and the generation of basaltic magmas in subduction zones below 200 km. The hydrated peridotite is formed by the slab-derived H_2O beneath the forearc region and is dragged downward by the subduction of oceanic lithosphere. Amphibole (Am) and chlorite (Chl) in the dragged hydrated peridotite layer decompose to release H_2O at around 110 km just beneath the volcanic front, while phlogopite (Ph) decomposes beneath the back arc side of a volcanic arc. Note that phlogopite in the lherzolite composition should be completely consumed at a depth of about 180 km according to the reaction; 2 phlogopite + diopside + 2 enstatite = K-amphibole + 2 pyrope + 2 forsterite + fluid (Sudo and Tatsumi, 1990). Thus, K-amphibole is likely the only hydrous phase

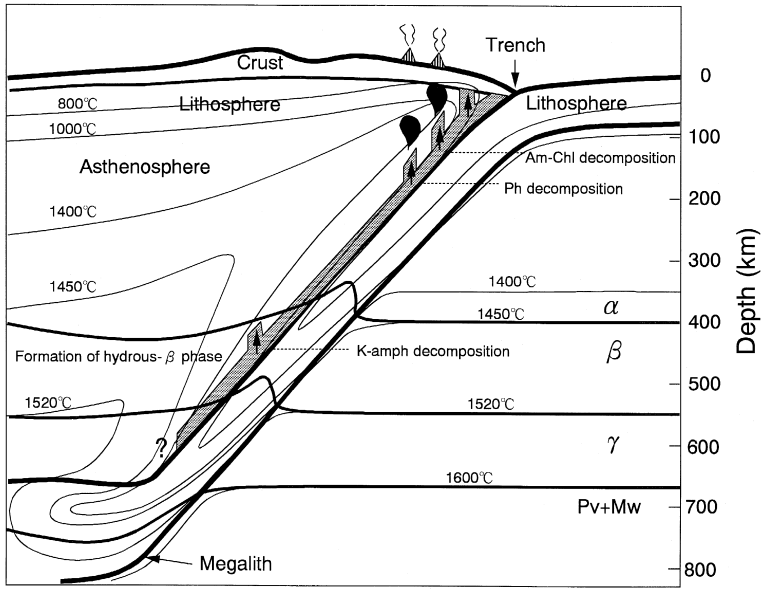

Fig. 6. A plausible model for the temperature distributions (Honda and Uyeda, 1983; Schubert et al., 1975; Tatsumi et al., 1983; Ito and Katsura, 1989) and the volcanic activities associated with the subducting slab. The latter model for the region below 200 km is after Tatsumi (1989). The present experiments suggest that K-amphibole is dehydrated at around 450 km in the dragged hydrous peridotite (shadow layer), which produces certain amounts of H_2O. However, the generated aqueous fluid reacts with β phase to form hydrous β-phase. Thus, the fluid is consumed by this reaction and the magmas associated with the dehydration cannot be generated by the decomposition of K-amphibole. Slab stagnation at 670 km discontinuity and the formation of megalith was suggested by Ringwood and Irifune (1988) and was later confirmed by a seismic tomography study (Fukao et al., 1992). The new hydrous phase (X, see text) may transport some amount of H_2O into these depth regions.

in the hydrous peridotite at depths greater than 180 km.

The present experiments demonstrate that the further dehydration of the dragged peridotite should occur at around 450 km by the decomposition of K-amphibole. However, the coexistence of β-phase confines the released H_2O in the transition region, as discussed above. Thus, H_2O-enriched layer is formed in this region of the mantle, and the third volcanic chain cannot be produced by the similar mechanism as advocated by Tatsumi (1989), except for possible unusually high temperature regions above ~ 1400°C at shallower than a 400-km depth, where K-amphibole dehydrates and no other hydrous phases are likely to exist.

The new hydrous phase (X) may bring certain amounts of H_2O into the deeper part of the mantle. The crystallographic nature and the stability limit of this phase should be further explored to address the transportation and circulation of H_2O throughout the entire mantle.

Acknowledgements

The authors thank T. Kawasaki, Y. Tatsumi, D.J. Weidner for valuable comments and D. Canil and an anonymous reviewer for constructive review. The authors are also grateful to K. Kuroda, M. Mizobuchi and M. Miyashita of Ehime University for technical assistance in the pressure calibrations. This study was supported by a fellowship program by the Inoue foundation for Promotion of Science.

References

Akaogi, M., Navrotsky, A., 1984. The quartz–coesite–stishovite transformations: new calorimetric measurements and calculation of phase diagrams. Phys. Earth Planet. Int. 36, 124–134.

Akaogi, M., Ito, E., Navrotsky, A., 1989. Olivine-modified spinel–spinel transitions in the system Mg_2SiO_4–Fe_2SiO_4: calorimetric measurements, thermodynamic calculation, and geophysical application. J. Geophys. Res. 94, 15671–15685.

Edwards, C., Menzies, M., Thirlwall, M., 1991. Evidence from Muriah, Indonesia, for the interplay of supra-subduction zone and intraplate processes in the genesis of potassic alkaline magmas. J. Petrol. 32, 555–592.

Foley, S., 1991. High-pressure stability of fluor- and hydroxy-endmembers of pargasite and K-richterite. Geochim. Cosmochim. Acta 55, 2689–2694.

Fukao, Y., Obayashi, M., Inoue, H., Nenbai, M., 1992. Subducting slabs stagnant in the mantle transition zone. J. Geophys. Res. 97, 4809–4822.

Gasparik, T., 1990. A thermodynamic model for the enstatite–diopside join. Am. Mineral. 75, 1080–1091.

Honda, S., Uyeda, S., 1983. Thermal process in subduction zones —a review and preliminary approach on the origin of arc volcanism. In: Shimozuru, D., Yokoyama, I. (Eds.), Arc Volcanism: Physics and Tectonics. Terra Scientific, Tokyo, pp. 117–140.

Huebner, J.S., Papike, J.J., 1970. Synthesis and crystal chemistry of sodium–potassium richterite, $(Na,K)NaCaMg_5Si_8O_{22}(OH,F)_2$: a model for amphiboles. Am. Mineral. 55, 1973–1992.

Inoue, T., 1994. Effect of water on melting phase relations and melt composition in the system Mg_2SiO_4–$MgSiO_3$–H_2O up to 15 GPa. Phys. Earth Planet. Int. 85, 237–263.

Inoue, T., Sawamoto, H., 1992. High-pressure melting of pyrolite under hydrous condition and its geophysical implications. In: Syono, Y., Manghnani, M.H. (Eds.), High-Pressure Research: Application to Earth and Planetary Sciences. Terra Scientific, Tokyo, and AGU, Washington, DC, pp. 315–322.

Inoue, T., Yurimoto, H., Kudoh, Y., 1995. Hydrous modified spinel, $Mg_{1.75}SiH_{0.5}O_4$: a new water reservoir in the mantle transition region. Geophys. Res. Lett. 22, 117–120.

Ito, E., Katsura, T., 1989. A temperature profile of the mantle transition zone. Geophys. Res. Lett. 16, 425–428.

Katsura, T., Ito, E., 1989. The system Mg_2SiO_4–Fe_2SiO_4 at high pressures and temperatures: precise determination of stabilities of olivine, modified spinel, and spinel. J. Geophys. Res. 94, 15663–15670.

Miyagi, I., Yurimoto, H., 1995. Water content of melt inclusions in phenocrysts using secondary ion mass spectrometer. Bull. Volcanol. Soc. Jpn. 40, 349–355.

Ringwood, A.E., Irifune, T., 1988. Nature of the 650-km seismic discontinuity: implications for mantle dynamic and differentiation. Nature 331, 131–136.

Ryabchikov, I.D., Boettcher, A.L., 1980. Experimental evidence at high pressure for potassic metasomatism in the mantle of the Earth. Am. Mineral. 65, 915–919.

Schubert, G., Yuen, D.A., Turcotte, D.L., 1975. Role of phase transition in a dynamic mantle. Geophys. J. R. Astr. Soc. 42, 705–735.

Sudo, A., Tatsumi, Y., 1990. Phlogopite and K-amphibole in the upper mantle: implication for magma genesis in subduction zones. Geophys. Res. Lett. 17, 29–32.

Tatsumi, Y., 1989. Migration of fluid phases and genesis of basalt magmas in subduction zones. J. Geophys. Res. 94, 4697–4707.

Tatsumi, Y., Sakuyama, M., Fukuyama, H., Kushiro, I., 1983. Generation of arc basalt magmas and thermal structure of mantle wedge in subduction zones. J. Geophys. Res. 88, 5815–5825.

Tatsumi, Y., Furukawa, Y., Kogiso, T., Yamanaka, Y., Yokoyama, T., Fedotov, S.A., 1994. A third volcanic chain in Kamchatka: thermal anomaly at transform/convergence plate boundary. Geophys. Res. Lett. 21, 537–540.

Tronnes, R.G., Takahashi, E., Scarfe, C.M., 1988. Stability of K-richterite and phlogopite to 14 GPa. EOS 69, 1510–1511.

Yurimoto, H., Kurosawa, M., Sueno, S., 1989. Hydrogen analysis in quartz crystals and quartz glasses by secondary ion mass spectrometry. Geochim. Cosmochim. Acta 53, 751–755.